

# Photoelectrochemical characteristics of CuIn<sub>0.5</sub>Ga<sub>0.5</sub>Se<sub>2</sub> films

M. Balasubramanian<sup>1</sup>, K. R. Murali<sup>2</sup>

<sup>1</sup>Vivekananda Institute of Professional Studies, Au Block, Pitampura, Delhi, India

<sup>2</sup>Department of Theoretical Physics, University of Madras, Chennai, India

Email of Corresponding Author : [muraliramkrish@gmail.com](mailto:muraliramkrish@gmail.com)

**Abstract**— CuIn<sub>0.5</sub>Ga<sub>0.5</sub>Se<sub>2</sub> films were pulse electrodeposited on molybdenum substrates at room temperature and at 50 % duty cycle. The total deposition time was 10 min. The films exhibited single phase chalcopyrite structure. Magnitude of the room temperature resistivity, mobility and carrier concentration were 4.85 ohm cm, 26.0 cm<sup>2</sup>V<sup>-1</sup>s<sup>-1</sup> and 4.95 x 10<sup>16</sup> cm<sup>-3</sup> respectively. Photoelectrochemical cells fabricated using the films indicates V<sub>oc</sub> of 0.70V, J<sub>sc</sub> of 18.0 mA cm<sup>-2</sup>, ff of 0.71 and η of 12.78 %, for 70 mW cm<sup>-2</sup> illumination after 70 s photoetching.

**Index Terms**—semiconductors, thin films, electronic material

## I. INTRODUCTION

In the recent years, polycrystalline solar cells based on CuInGaSe<sub>2</sub> (CIGS) have gained importance [1-3]. CIGS has shown to be a promising candidate as an absorber material for thin film solar cells. Efficiencies near 19% have been reached on a laboratory scale. Several technique like co-evaporation [4,5], selenization of metallic precursors [6,7], nano-ink printing [8] and electrodeposition [9] have been developed for the preparation of CIGS absorbers. In this work CIGS thin films have been obtained by the pulse electrodeposition technique.

In pulse electrodeposition [10,11] the potential or current is alternated swiftly between two different values. This results in a series of pulses of equal amplitude, duration and polarity, separated by zero current. Each pulse consists of an ON-time (T<sub>ON</sub>) during which potential and current is applied, and an OFF-time (T<sub>OFF</sub>) during which zero current is applied as shown in Fig. 1. It is possible to control the deposited film composition and thickness in an atomic order by regulating the pulse amplitude and width. They favor the initiation of grain nuclei and greatly increase the number of grains per unit area resulting in finer grained deposit with better properties than conventionally plated coatings. The sum of the ON and OFF times constitute one pulse cycle. The duty cycle is defined as follows:

$$\text{Duty Cycle (\%)} = \frac{(\text{ON time})}{(\text{ON time} + \text{OFF time})} \times 100 \quad (1)$$

A duty cycle of 100% corresponds to conventional plating because OFF time is zero. In practice, pulse plating usually involves a duty cycle of 5% or greater. During the ON time the concentration of the metal ions to be deposited is reduced within a certain distance from the cathode surface. This so-called diffusion layer pulsates with the same frequency as the applied pulse current. Its thickness is also related to ip but reaches a limiting value governed primarily by the diffusion coefficient of the metal ions. During the OFF time the concentration of the metal ions build up again by diffusion from the bulk electrolyte and will reach the equilibrium concentration of the bulk electrolyte if enough time is allowed. These variables result in two important characteristic features of pulse plating which make it useful for alloy plating as well as property changes as mentioned earlier.

(i) Very high instantaneous current densities and hence very high negative potentials can be reached. The high over potential causes a shift in the ratio of the rates of reactions with different kinetics. This high over potential associated with the high pulse current density greatly influences the nucleation rate because a high energy is available for the formation of new nuclei.

(ii) The second characteristic feature is the influence of the OFF time during which important adsorption and desorption phenomena as well as recrystallization of the deposit occurs.

Pulse plating technique has distinct advantages compared to conventional electrodeposition namely, crack free, hard deposits and fine grained films with more uniformity, lower porosity and better adhesion. It is well known that by using pulse current for electrodeposition of metals and alloys it is possible to exercise greater control over the properties of electrodeposits and to improve them by modifying their microstructures [12].

## II. EXPERIMENTAL METHODS

CuIn<sub>0.5</sub>Ga<sub>0.5</sub>Se<sub>2</sub> films were pulse electrodeposited on molybdenum substrates at 50 % duty cycle and at room temperature. The precursors used were 20 mM SeO<sub>2</sub>, 30 mM CuCl<sub>2</sub>, 50 mM Indium chloride and 50 mM gallium chloride. The deposition potential was maintained at -0.8V (SCE). The pH was maintained at 1.5 by HCl. A microprocessor controlled pulse plating unit was used. Thickness of the films measured by Mitutoyo surface profilometer was 900 nm. The films were characterized by Xpert analytical x-ray diffraction unit with Cu Kα radiation. Optical measurements were recorded using an Hitachi UV-VIS-IR spectrophotometer. Composition of the films was estimated by EDAX attachment to JOEL SEM. Electrical measurements were made by Hall Van der Pauw method. Photoelectrochemical cell measurements were made with 250 W tungsten halogen lamp, load resistance box, Digital multimeters for measuring current and voltage output.

## III. RESULTS AND DISCUSSION

Microstructural parameters were estimated by studying the x-ray diffractograms of CuIn<sub>0.5</sub>Ga<sub>0.5</sub>Se<sub>2</sub> films.

Fig.1 shows the x-ray diffraction patterns of  $\text{CuIn}_{0.5}\text{Ga}_{0.5}\text{Se}_2$  films. All the figures indicate the prominent peaks corresponding to (112), (220)/(204), (312)/(116). These are characteristic of the chalcopyrite phase. No other phases were observed in the x-ray diffractograms indicating the formation of single phase material. The lattice parameters were calculated using the following relation [13]

$$1/d^2 = (h^2 + k^2)/a^2 + l^2/c^2 \dots\dots\dots(1)$$

Where, 'a' and 'c' are the lattice parameters, "d" is the lattice spacing. The estimated values of 'a' and 'c' are 5.693 and 11.330 respectively.

The crystallite size of the films have been calculated using Scherrer's formula [14],

$$D = 0.94\lambda / \beta \cos\theta \dots\dots\dots(2)$$

where  $\lambda$  is the wavelength of X-ray used,  $\beta$  the full-width half-maximum (FWHM) and  $\theta$  the Bragg angle. The crystallite size was 50 nm. The dislocation density  $\delta$ , defined as the length of dislocation lines per unit volume of the crystal has been evaluated using the formula [15]

$$\delta = 1/D^2 \dots\dots\dots(3)$$

Information on the particle size and strain for the films was obtained from the full-width at half-maximum of the diffraction peaks. The full-width at half-maximum  $\beta$  can be expressed as a linear combination of the contributions from the particle size, D and strain,  $\epsilon$  through the relation [16]

$$\beta \cos\theta / \lambda = 1/D + \epsilon \sin\theta / \lambda \dots\dots\dots(4)$$

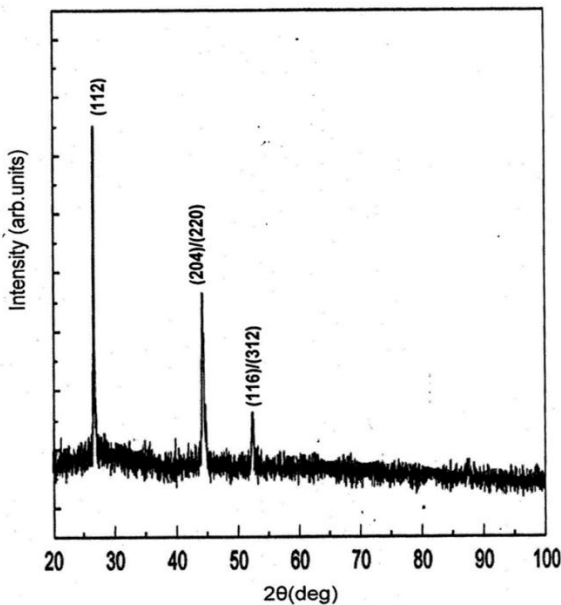


Figure.1 : X-ray diffraction pattern of  $\text{CuIn}_{0.5}\text{Ga}_{0.5}\text{Se}_2$  films deposited at 50 % duty Cycle

The plot of  $\beta \cos\theta / \lambda$  vs  $\sin\theta / \lambda$  allows us to determine both strain and particles size from slope and intercept of the graph. The estimated values of strain for the films is  $1.87 \times 10^{-4}$ . The value of dislocation density was  $0.37 \times 10^{15}$  lines  $\text{cm}^{-3}$ . The above parameters were

estimated by the built in software of the x0rqaq diffraction unit.

Composition of the films was estimated by recording the EDS spectrum of the films deposited of different composition. Fig.2 shows the EDS spectrum of  $\text{CuIn}_{0.5}\text{Ga}_{0.5}\text{Se}_2$  films. Based on the defect chemistry model of ternary compounds [17], compositional deviations of the  $\text{CuIn}_{0.5}\text{Ga}_{0.5}\text{Se}_2$  films can be expressed by non-stoichiometry parameter ( $\Delta y = [2\text{Se}/\{\text{Cu} + 3(\text{Ga} + \text{In})\}] - 1$ ). The parameter  $\Delta y$  is related to the electronic defects. For  $\Delta y > 0$ , the film has a p-type conductivity and it has an n-type conductivity for  $\Delta y < 0$ . In this study the value of  $\Delta y$  is greater than zero and the films exhibit p-type conductivity. The composition of the film was Cu (24.20 %), In (12.00 %), Ga (12.00 %) and Se ( 51.80 %); Cu/(Ga + In) ratio was 1.01; and the value of  $\Delta y = 2\text{Se}/\{\text{Cu} + 3(\text{Ga} + \text{In})\} - 1$  value was 1.07, since this value is greater than unity, the films exhibit p-type behaviour.

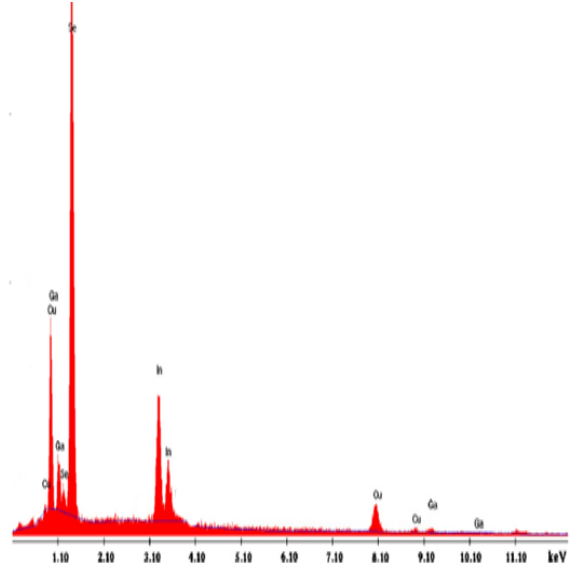


Figure.2: EDS spectrum of  $\text{CuIn}_{0.5}\text{Ga}_{0.5}\text{Se}_2$  films deposited at 50 % duty cycle

The room temperature transport parameters were measured by Hall Van der Pauw technique by providing gold ohmic contact. The magnitude of the room temperature resistivity was 4.85 ohm cm, the value of the room temperature mobility was  $26.0 \text{ cm}^2\text{V}^{-1}\text{s}^{-1}$  and the room temperature carrier concentration was  $4.95 \times 10^{16} \text{ cm}^{-3}$ . The resistivity values are comparable with an earlier report [18]. The Cu/(Ga + In) ratio is greater than unity. The films exhibit p-type conductivity. This is supported by the EDAX measurement.

Photoelectrochemical cells (PEC) cells using these films exhibited low photocurrent and photovoltage. The intensity of the light falling on the films was kept constant at  $70 \text{ mW cm}^{-2}$ . The as deposited film exhibited low photo output viz.,  $V_{oc}$  of 0.25 V and  $J_{sc}$  of  $80 \mu\text{A cm}^{-2}$ , hence, in order to increase the photo output, the films were post heated in argon atmosphere at different temperatures in the range of 450 - 550°C for 15 min. Fig.3 shows the load characteristics of the post heat treated films of composition  $\text{CuIn}_{0.5}\text{Ga}_{0.5}\text{Se}_2$ . From the figure, it is observed that the PEC output parameters, viz., open circuit voltage and short circuit current were found to increase for the electrodes heat-treated upto a temperature

of 525°C. Photoelectrodes heat-treated at temperatures greater than this value exhibited lower open circuit voltage and short circuit current due to the reduction in thickness of the films as well as the slight change in stoichiometry. The photovoltaic parameters are  $V_{oc}$  of 0.55 V and  $J_{sc}$  of 10.5 mA cm<sup>-2</sup>, ff of 0.72, efficiency of 5.94 %.

It was observed that both  $V_{oc}$  and  $J_{sc}$  increased with increase of intensity. Beyond 80 mW cm<sup>-2</sup> illumination,  $V_{oc}$  was found to saturate as is commonly observed in the case of photovoltaic cells and PEC cells,  $J_{sc}$  is found to linearly increase with intensity of illumination. A plot of  $\ln J_{sc}$  vs  $V_{oc}$  yielded a straight line. Extrapolation of the line to the y-axis yields a  $J_0$  value of  $1.30 \times 10^{-7}$  A cm<sup>-2</sup>, the ideality factor ( $n$ ) was calculated from the slope of the straight line and it was found to be 1.95.

Photoetching was done by shorting the photoelectrodes and the graphite counter electrode under an illumination of 100 mW cm<sup>-2</sup> in 1 : 100 HNO<sub>3</sub> for different durations in the range 0 – 100s. Both photocurrent and photovoltage are found to increase up to 70s photoetch, beyond which they begin to decrease. This is illustrated in Fig.4 for the CuIn<sub>0.5</sub>Ga<sub>0.5</sub>Se<sub>2</sub> photoelectrode after post heat treatment. The decrease of the photocurrent and photovoltage after 70s photoetch is attributable to separation of grain boundaries due to prolonged photoetching [19]. The power output characteristics (Fig.5) after 70s photoetching indicates a  $V_{oc}$  of 0.70V,  $J_{sc}$  of 18.0 mA cm<sup>-2</sup>, ff of 0.71 and  $\eta$  of 12.78 %, for 70 mW cm<sup>-2</sup> illumination.

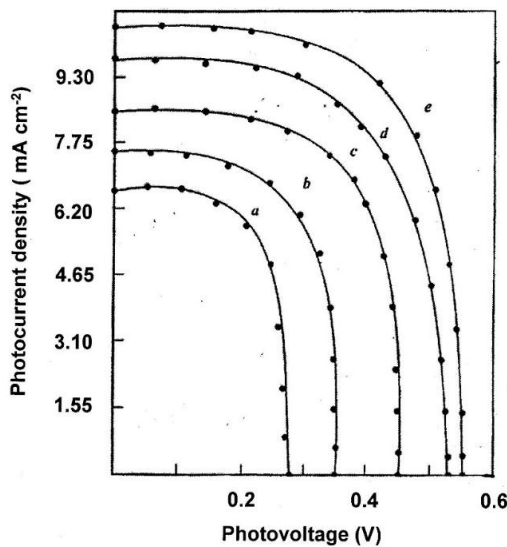


Figure 3 : Load characteristics of CuIn<sub>0.5</sub>Ga<sub>0.5</sub>Se<sub>2</sub> films deposited at 50 % duty cycle and post heat treated at different temperatures (a) 450°C (b) 475°C (c) 500°C (d) 525°C (e) 550°C

Photoetching process successfully decreases the density of recombination centers by etching out surface steps and imperfections. This leads to improvement in photocurrent (the maximum observed increase in photocurrent was by more than 3 times and hence conversion efficiencies. It was found that surface steps, inhomogenities and defects are etched/removed as a result of photoetching. The photoetching process has been generally found to result in a slight increase in the

photovoltage (open circuit voltage). This has been found to be a consequence of the change in flat band potential.

Photoetching is apparently one of the most promising surface treatment process for enhancement of conversion efficiency through suppression of recombinations. The fill factor (FF) is another important PEC parameter which manifests the solar-to-electrical energy conversion efficiency of the cell. It reflects the ability of photogenerated current to perform work through an external load and is therefore very sensitive to the kinetics of current flow through the semiconductor/electrolyte interface. It has been found that in addition to photocurrent, the fill factor gets enhanced, but to a lesser degree as a result of photoetching. The dominant reason for this is thought to be a decrease in recombination velocity of minority carriers. The improvement in the fill factor indicates the fact that the semiconductor/electrolyte interface behaves closer to the ideal case after photoetching, i.e., the dark saturation current decreases (shunt resistance increases), (series resistance decreases). A side result of photoetching is a decrease in reflectivity and hence an increase in absorptivity of light leading to a better conversion efficiency. It is thought that the decrease in reflectivity occurs due to the formation of microetch pits on the electrodes and hence a roughening of the surface steps upon photoetching. Similar behaviour was observed in WSe<sub>2</sub> photoelectrodes [20].

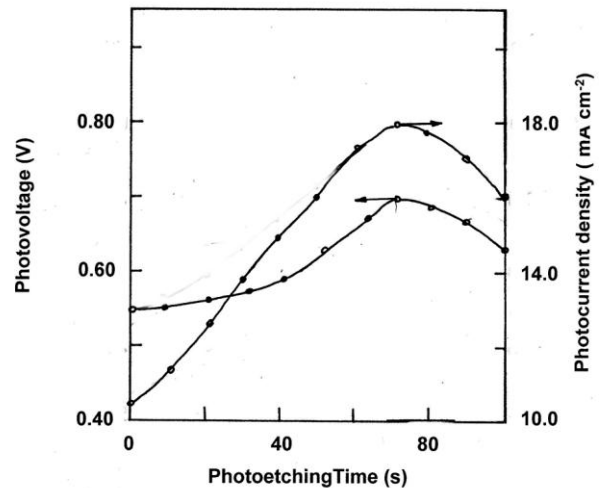


Figure 4 : Variation of  $V_{oc}$  and  $J_{sc}$  of CuIn<sub>0.5</sub>Ga<sub>0.5</sub>Se<sub>2</sub> films deposited at 50 % duty cycle and post heat treated at 525°C with photoetching time

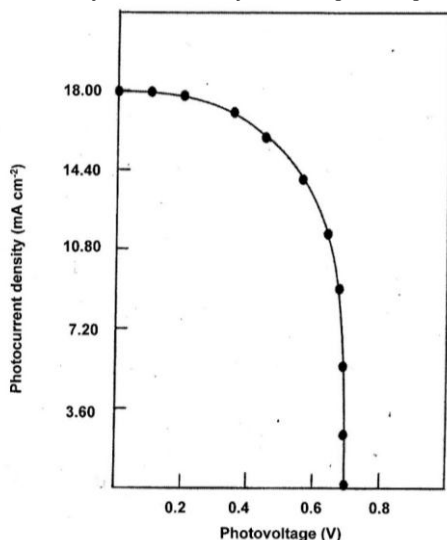


Figure.5 : Load characteristics of  $\text{CuIn}_{0.5}\text{Ga}_{0.5}\text{Se}_2$  films deposited at 50 % duty cycle and post heat treated at  $525^\circ\text{C}$  after photoetching for 70s.

#### IV. CONCLUSIONS

$\text{CuIn}_{0.5}\text{Ga}_{0.5}\text{Se}_2$  films possessing chalcopyrite structure with crystallite size of 50 nm can be deposited by the pulse electrodeposition technique. Single phase films can be obtained. Room temperature resistivity of the films was 4.85 ohm cm. The films exhibited photoactivity. Photoelectrochemical cells fabricated with the films have exhibited efficiencies above 12 %. Further improvements can be made by further reducing the resistivity.

#### REFERENCES

[1] P. Reinhard, S. Buecheler, A.N. Tiwari, "Technological status of  $\text{Cu}(\text{In}, \text{Ga})(\text{Se}, \text{S})_2$ -based Photovoltaics". *Sol. Energy Mater. Sol. Cells.*, 119, : 287–290, 2013

[2] T. Nakada, "CIGS-based thin film solar cells and modules: unique material properties". *Electron. Mater. Lett.* 8, 179–185, 2012

[3] M.A. Green, K. Emery, Y. Hishikawa, W. Warta, D. Dunlop, "Solar cell efficiency tables", *Prog. Photovolt: Res. Appl.* 22, 1–9, 2014

[4] C. Xu, H. Zhang, J. Parry, S. Perera, G. Long, H.A. Zeng, "Single source three-stage evaporation approach to CIGS sorber layer for thin film solar cells". *Sol. Energy Mater. Sol. Cells.* 117, 357–362, 2013

[5] F. Pianezzi, P. Reinhard, A. Chirilă, S. Nishiwaki, B. Bissig, S. Buecheler, A.N. Tiwari, "Defect formation in  $\text{Cu}(\text{In}, \text{Ga})\text{Se}_2$  thin films due to the presence of potassium during growth by low temperature co-evaporation process". *J. Appl. Phys.* 114, :194508, 2013

[6] W. Li, Y. Sun, W. Liu, Z. Zhou, "Fabrication of  $\text{Cu}(\text{In}, \text{Ga})\text{Se}_2$  thin films solar cell by selenization process with Se vapor". *Sol. Energy.* 80, 191–195, 2006

[7] Baji, Z. Lábadi, G. Y. Molnár, B. Pécz, A. L. Tóth, J. Tóth, A. Cisik, I. Bársony, "Post-selenization of stacked precursor layers for CIGS". *Vacuum*, 92, 44–51, 2013

[8] S. J. Park, J. W. Cho, J. K. Lee, K. Shin, J. Kim, B. K. Min, "Solution processed high band-gap  $\text{CuInGaS}_2$  thin film for solar cell applications". *Prog. Photovolt: Res. Appl.* 22, 122–128, 2014

[9] C. Lee, I. Choi, V. S. Saji, "Progress in electrodeposited absorber layer for  $\text{CuIn}_{(1-x)}\text{Ga}_x\text{Se}_2$  (CIGS) solar cells". *Sol. Energy.* 85, 2666–2678, 2011

[10] M. Ghaemi, I. Binder, "Effect of direct and pulse current of Manganese Dioxide". *J. Power Sources.* 111, 248–254, 2002

[11] A. Marlot, P. Kern, D. Landolt, "Pulse plating of Ni-Mo Alloys from Ni rich electrolytes", *Electrochim Acta*, 48, 29–36, 2002

[12] M. E. Bahrololoom, R. Sani, "Influence of pulse plating parameters on the hardness and wear resistance properties of Ni-alumina coatings", *Surf. coat. tech.* 192, 154–163, 2005

[13] M. F. C. Ladd, R. A. Palmer, "Structure determination by x-ray crystallography", 3<sup>rd</sup> Ed, Plenum Press, New York, 1993.

[14] C. A. Rincon, E. Hernandez, M. T. Alanso, M. Garriza, S. M. Wasim, C. Rincon, M. Leon, "Optical transitions near the band edge in gulk  $\text{CuInGaSe}_2$  by ellispometric Measurements", *Mater. Chem. Phys.* 70, 300–304, 2001.

[15] H. Mustafa, D. Hunter, A. K. Pradhan, U. N. Roy, Y. Cui, A. Burger, "Synthesis and characterization of  $\text{AgInSe}_2$  for thin film solar cells", *Thin solid films*, 515 : 7001–7004, 2007

[16] M. C. Santhosh Kumar, B. Pradeep, "Formation and properties of  $\text{AgInSe}_2$  thin films by co- evaporation. *Vacuum* 72, 369–378, 2004

[17] J. A. Groenik, P. H. Janse, "A generalized approach to defect chemistry of ternary Compounds, *Z. Phys. Chem.* 110, 17–28, 1978

[18] K. T. R. Reddy, R. B. V. Chalapathy, "Preparation and properties of sprayed  $\text{CuIn}_{0.6}\text{Ga}_{0.4}\text{Se}_2$  thin films. *Sol. Energy Mater. Sol. Cells.* 50, : 19–24, 1998

[19] J. P. Mangalhari, R. Thangaraj, O. P. Agnihotri, "Photoelectrochemical conversion using sprayed  $\text{CdSe}$ ", *Bull. Mater. Sci.* 10, 333–340, 1988

[20] G. Prasad, O. N. Srivastava, "The high efficiency (17.1 %)  $\text{WSe}_2$  photoelectrochemical solar cell" *J. Phys. D.*, 21, 1028–1030, 1988